

IAC-15-A2.6.2

RESULTS OF MICROGRAVITY FLUID DYNAMICS CAPTURED WITH THE SPHERES-SLOSH EXPERIMENT

**Gabriel Lapilli**

Florida Institute of Technology, USA, [glapilli2009@my.fit.edu](mailto:glapilli2009@my.fit.edu)

Dr. Daniel Kirk

Florida Institute of Technology, USA, [dkirk@fit.edu](mailto:dkirk@fit.edu)

Dr. Hector Gutierrez

Florida Institute of Technology, USA, [hgutier@fit.edu](mailto:hgutier@fit.edu)

Dr. Paul Schallhorn

NASA - Kennedy Space Center, USA, [paul.a.schallhorn@nasa.gov](mailto:paul.a.schallhorn@nasa.gov)

Mr. Brandon Marsell

NASA - Kennedy Space Center, USA, [brandon.marsell@nasa.gov](mailto:brandon.marsell@nasa.gov)

Mr. Jacob Roth

NASA - Kennedy Space Center, USA, [jacob.roth@nasa.gov](mailto:jacob.roth@nasa.gov)

Dr. Jeffrey Moder

NASA, USA, [jeffrey.p.moder@nasa.gov](mailto:jeffrey.p.moder@nasa.gov)

This paper provides an overview of the SPHERES-Slosh Experiment (SSE) aboard the International Space Station (ISS) and presents on-orbit results with data analysis. In order to predict the location of the liquid propellant during all times of a spacecraft mission, engineers and mission analysts utilize Computational Fluid Dynamics (CFD). These state-of-the-art computer programs numerically solve the fluid flow equations to predict the location of the fluid at any point in time during different spacecraft maneuvers. The models and equations used by these programs have been extensively validated on the ground, but long duration data has never been acquired in a microgravity environment. The SSE aboard the ISS is designed to acquire this type of data, used by engineers on earth to validate and improve the CFD prediction models, improving the design of the next generation of space vehicles as well as the safety of current missions. The experiment makes use of two Synchronized Position Hold, Engage, Reorient Experimental Satellites (SPHERES) connected by a frame. In the center of the frame there is a plastic, pill shaped tank that is partially filled with green-colored water. A pair of high resolution cameras records the movement of the liquid inside the tank as the experiment maneuvers within the Japanese Experimental Module test volume. Inertial measurement units record the accelerations and rotations of the tank, making the combination of stereo imaging and inertial data the inputs for CFD model validation.

## I. INTRODUCTION AND BACKGROUND

Sloshing problems are of increasing concern in a rocket upper-stage and spacecraft applications. In microgravity, the influence of sloshing liquid propellants may influence critical maneuvers such as docking of cargo vehicles or pointing of satellites. Severe problems with sloshing liquid in spacecraft have been reported. As an example of the potential slosh impact on rocket performance, a pre-launch review of the Computational Fluid Dynamics (CFD) propellant slosh predictions within the second-stage of a Delta IV launch vehicle led to a launch stand down until the issue could be resolved. The CFD predictions from the same tool varied significantly depending on whether a 4 or 6-Degree of Freedom (DOF) model was used. A worst case scenario predicted that the liquid hydrogen would not remain constrained in the aft end of the tank and could be ingested into the tank vent-and-relief system resulting in a thrust imbalance and loss of vehicle control. The

analysis team concluded that it was imperative to “determine proper methodology for future Delta IV second-stage propellant slosh analysis”<sup>1</sup>. In another example, the NEAR satellite went into safety mode because of an unexpected reaction that was possibly due to propellant slosh after an orbital maneuver which caused a one year delay of the project<sup>2</sup>. Finally, recently in March of 2007, SpaceX Falcon 1 vehicle tumbled out of control<sup>3</sup>. An oscillation appeared in the upper stage control system approximately 90 seconds into the burn and instability grew in pitch and yaw axes initially and after about 30 seconds also induced a noticeable roll torque. This roll torque eventually overcame the second stage roll control thrusters and centrifuged propellants, causing flame-out of the Kestrel engine. There is high confidence that LOX slosh was the primary contributor to this instability. This conclusion has been verified by third party industry experts that have reviewed the flight telemetry<sup>4</sup>.

The SPHERES-Slosh Experiment (SSE) was built by Florida Institute of Technology to investigate in the matter. It makes use of two Synchronized Position Hold, Engage, Reorient Experimental Satellites (SPHERES), connected by a frame. Multiple plastic pill shaped tanks partially filled with water are used, with fill fractions of 20%, 40% and a solid mass replicator, representing the 40% fill fraction tank evenly distributed. High resolution cameras record the movement of the liquid inside the tank as the experiment maneuvers within the ISS test volume, either driven by SPHERES or manually by the crewmember. Inertial measurement units record the accelerations of the tank, making the combination of stereo imaging and inertial data the inputs for CFD model validation.

## II. SPHERES-SLOSH EXPERIMENT OVERVIEW

The primary objective of the SPHERES Slosh Experiment (SSE), depicted in Fig. 1, is to acquire long duration, low-gravity liquid slosh data aboard the International Space Station<sup>5</sup>.



Fig. 1: Flight Engineer Richard Mastracchio with the SSE onboard the KIBO module of the ISS.

The core of the SSE consists of a partially filled (with water) transparent tank fitted to a structural frame and two cameras (in orthogonal configuration) recording the liquid distribution, shown in Fig. 2. Two sets of Inertial Measurement Units (IMUs) are used to record the inertial measurements. The SSE utilizes the manifested SPHERES laboratory and will use the VERTIGO platform (already on-board the ISS). The SPHERES units propel the SSE and the VERTIGO units are used to record the captured IMU/camera data on its local hard drives. Adequate lighting for image capture is provided via LED panels, installed within the Backdrop and Hood. The Slosh Avionics Box contains the IMUs and also

provides power to the Camera and the LED panels through the VERTIGO unit. Each of the Slosh Avionics Boxes connects to a VERTIGO unit. The VERTIGO-Slosh Avionics Box packages then connect to the SPHERES units via the SPHERES expansion port. Each SPHERES unit resides within the Frame Arm saddles and is clamped down during the SSE operation. During test sessions, different maneuvers are performed, based on the specific science needs set for the session. These maneuvers include investigation of a wide variety of microgravity slosh phenomena, from CFD correlations to advanced space vehicle maneuvers, planned along with both government agencies and commercial partners.

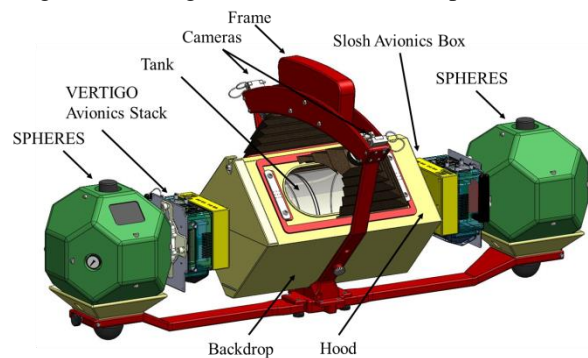


Fig. 2: SSE perspective view, showing main components

Three former papers have been published with design details of the SSE. References <sup>6</sup> and <sup>7</sup> provide detailed design characteristics regarding fluid and maneuver scaling, as well as non-dimensional mapping of full-scale and downsized executed maneuvers. Reference <sup>8</sup> provides a detailed approach on material selection and non-fluid related design choices, including flight certification requirements and testing criteria.

## III. ISS SCIENCE DEVELOPMENT

A total of nine science sessions are being executed onboard the ISS. By August 2015, 5 science sessions have been completed, with three more planned. Table 1 summarizes the dates and tanks used for each of the sessions.

Session	Tank	Date
Checkout	40%	Jan 22, 2014
Science 1	40%	Feb 28, 2014
Science 2	20%	Jun 18, 2014
Science 3	20%	Sep 09, 2014
Science 4	40%	Jul 17, 2015
Science 5	40%	Aug 07, 2015
Science 6	40%	September, 2015
Science 7	TBD	TBD
Science 8	TBD	TBD

Table 1: Slosh sessions

The first session consisted in a full checkout of the experiment, inspecting for potential damage to the payload during transportation to the ISS, as well as a first back of data runs. Science sessions 1, 2 and 3 targeted optimization of the data, with an emphasis on creating proper initial conditions for the fluid.

In order for the data to be useful for validating and anchoring CFD models, the maneuvers must begin with the fluid in a configuration that is uncomplicated and easily reproduced. Overly complex initial conditions cannot be accurately reproduced in CFD, causing the simulation to be inaccurate. **Error! Reference source not found.** is an example of the initial condition of the fluid in the tank during the checkout session. The fluid is not uniformly distributed within the tank and a large number of air bubbles are scattered throughout. Accurately representing this condition using CFD is not feasible.

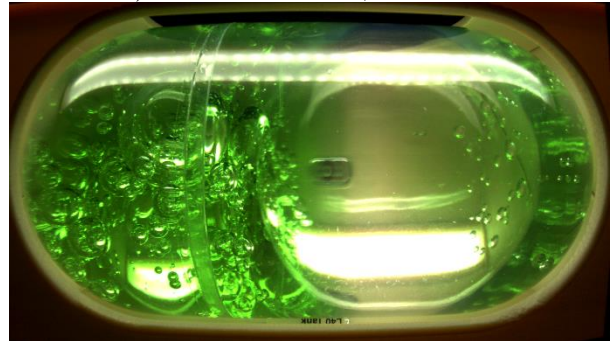
After realizing that the initial condition in the tank is not conducive to CFD validation, it was decided that any future sessions would attempt to remove the bubbles and create a less complicated initial condition. After the checkout session was completed, the team set out to resolve the initial conditions problem by developing maneuvers that should cause the air to separate from the liquid and develop a good initial condition.

The next test session was called Science 1 as it would serve as the first session with gathering science data as the primary objective. For this session, a total of three maneuvers were developed to attempt to produce a better initial condition. The crew members running the session were instructed to try all three and determine which works best. The first maneuver involved accelerating the system along the principal (long) axis and quickly bringing it to a stop. The second method involved spinning the experiment about one of the SPHERES. Both of these methods were fairly effective but required a large amount of space which is not readily available on the ISS. The third method turned out to be the preferred method as it took less space and proved to be most effective. This method involved spinning the system about its center axis. When the crew members did this initialization maneuver by hand, the fluid would cleanly split in two and make a nice initial condition. Fig. 3 illustrates the difference between a bad initial condition, as seen during the checkout session, and a good initial condition as seen after implementing the initialization maneuver.

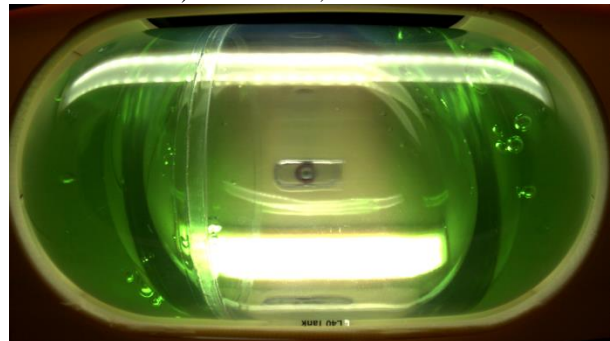
Science 1 was a very productive session that used the 40% tank. This session successfully completed 11 runs. Several of these runs were completed with the light box removed so the crew members could monitor how well the initialization maneuvers worked. Once the fluid was properly initialized, the crew members were instructed to initiate the thruster firing sequence. A majority of the

runs completed during this session involved thruster firings from the SPHERES.

a) Checkout Session, 40% tank



b) Science 1, 40% tank



c) Science 2, 20% tank

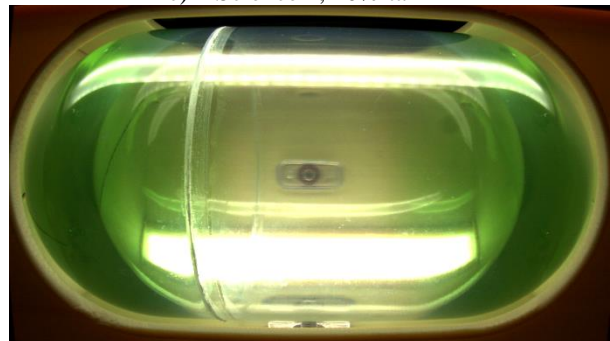


Fig. 3: Evolution of initial conditions through the first three science sessions

Post processing of the data from this session revealed that:

- The acceleration levels achieved by the thrusters on the SPHERES are simply too low to create any significant fluid motion. Since the validation of the CFD tools require fluid motion, the data quality from this session was rather low.

- The crew members were capable of pushing the system in a way that created interesting fluid motion in the tank. The higher acceleration levels achieved by manually moving the experiment created higher quality data.

Since the low levels of thrust from the SPHERES were determined to be insufficient to properly move the

fluid in the tank, the following session was designed to include more runs with crew induced maneuvers.

Science 2 was the first session to use the 20% fill fraction tank, denominated L20, and the same settling principles found for the 40% tank (L40) were applied to this session, as shown in Fig. 3c). It consisted of several tests under rotational, translational and pitching motions.

Science 3, performed with the L20 tank (20% fill fraction), contained a few specific maneuvers on satellite deployment issues.

Science 4 was focused on replicating the same maneuvers from Science 3, using the 40% tank instead.

As shown in Fig. 3a, b and c, no meniscus is visible in the tank, suggesting a fully wetted inner surface. This triggered particular interest to find the transition value of Bond number between a fully surface-tension dominated regime to an inertial-dominated regime, through the observation of the meniscus. During Science session 5 crewmembers were asked to perform maneuvers manually outside the slosh frame and provide visual feedback on the transition characteristics.

#### IV. ISS RESULTS AND MODELING

##### Inertia Estimation

One of the main accomplishments of the Checkout session included the verification of thruster performance as well as inertia values. On earth, under normal gravity, it is difficult to accurately measure the inertia of a system like the slosh experiment. By commanding the experiment to rotate about each of the main axes, and measuring the rotation rates achieved, a much more accurate value of the inertia tensor is theoretically possible. In practice however, it is a difficult task. During the checkout session there were several maneuvers that yielded unexpected motions in the system.

Using Newton's law of motion, the inertia of a system can be calculated using the following equation (1).

$$\tau = I \alpha \quad (1)$$

Where  $\tau$  is the input torque on the system,  $\alpha$  is the measured angular acceleration, and  $I$  is the moment of inertia about the axis of rotation. Though at first look it seems simple to calculate, in practice the exercise is fairly complex.

The gyrometers on the system measure angular velocity (in degrees per second) and self calibrate every time the unit is powered on. This means that the system needs to be perfectly still every time the self calibration occurs, otherwise there will be a bias in the signal. Since this is very difficult to do in zero gravity, the biases had to be removed in post processing. Once all of the biases were removed, the angular acceleration needed to be calculated. This was done by numerically integrating the angular velocity signal from the gyrometers. As is common, the further along in time, the more integration

error gets accumulated. This causes the angular acceleration to not be as accurate as the raw angular velocity measurements. However, most of these errors were taken into account and a good estimate of the angular acceleration was calculated.

In order to calculate the applied torque, the total thrust applied by the thrusters on the SPHERES needed to be extracted from the data as well. Though these thruster values were fairly well known when the system was first flown to the ISS, after roughly 10 years aboard the ISS the thruster performance has changed. Since the total mass of the system was accurately measured before launch, it was possible to back-out thruster forces from measured accelerations. There are a total of 12 thrusters per SPHERE and the system uses an average of 4 thrusters at a time on any given maneuver. Since only 12 runs were completed, and out of those twelve less than half involved some sort of linear acceleration, it was impossible to characterize the thrust profile of every single thruster on the system. Instead, an attempt was made to characterize the thrust from different sets of thrusters and calculate an average value. After completing this analysis, the thrust value (per thruster) was estimated to be within a range of 0.066 N to 0.17 N.

Using this range of thruster values along with the estimated angular acceleration signal, the moments of inertia of the system were computed. The results of this analysis are shown in Table 2, compared to the calculated moments of inertia using CAD prior to launch.

Table 2: Experimental moments of inertia (kg m<sup>2</sup>)

Moment of Inertia	Minimum	Maximum	Average	CAD Calculated
I <sub>xx</sub>	0.145	0.410	0.2775	0.3151
I <sub>yy</sub>	1.186	3.360	2.273	2.5471
I <sub>zz</sub>	1.096	3.104	2.100	2.4326

Since the expected moments of inertia values were well within the range of values derived from the flight data, it was determined that the unexpected movements were not caused by an error in the moments of inertia. Instead, the flight data pointed toward unexpected variations in the thrusters on the SPHERES.

##### CFD Modeling and Comparison

Science 3 included a maneuver to replicate a particular satellite deployment problem, in which a spring-load deployment system induces a thrust pulse in the longitudinal direction of the tank, creating a slosh wave traveling along the tank. This scenario was recreated by having the crewmember push the experiment in the same manner, with the 20% tank settled in both hemispheres. The recorded acceleration curve was applied as a mesh motion boundary condition to a CFD model created in STAR-CCM+. Due to confidentiality constraints of the data, the acceleration curve, the timestamps of the images and the model

characteristics cannot be released. Acceleration levels are shown qualitatively as the magnitude of the arrow on top of each frame in Fig. 4.

Fig. 4a shows the initial condition of the liquid, both the real tank (top) and the CFD simulation (bottom, inner surface plotted green). This corresponds to the near minimum-energy state after settling, with the experiment free floating.

Fig. 4b shows the experiment being pulled by the crewmember, creating a fluid shift converging in the right hemisphere and initiating a blob. CFD model predictions display a similar behaviour, with a less pronounced blob generation, without a clear cause. Some potential causes may be:

- Mesh resolution
- Slight misalignment in the measured acceleration
- Slight difference in fill level (CFD vs real)
- Surface tension modeling

Fig. 4c displays a frame after the thrust pulse has been inverted and the fluid has shifted to the opposite side of the tank. The convergent inner geometry of the tank, combined with the momentum carried by the fluid, creates a central geyser that is replicated perfectly by CFD. Fig. 4d continues this effect, with a reducing acceleration that shrinks the base of the geyser. The CFD model was not able to capture this effect, potentially due to the same reasons explained above.

Fig. 4e shows the droplet detaching from the rest of the domain. The difference in positions, given that these two images correspond to the same time instant, can be explained by integration error and noise of the accelerometer readings, producing a velocity shift that translates into different distance travelled by the fluid.

Fig. 4f lastly displays the moment when the droplet impacts the opposite side of the tank and merges the fluid attached to the walls.

It is important to note that all frames display a slight green colouring on the entire tank and no meniscus is clearly visible, suggesting that a thin film is always coating the inner surface of the tank. CFD predictions simulate that behaviour perfectly at all times.

This type of study has been performed in many occasions and this is the first time it is appropriately recreated and recorded in real, microgravity conditions for scientific validation. Geysering is an adverse effect, heavily studied and mitigated by devices such as geyser limiting baffles<sup>9</sup>.

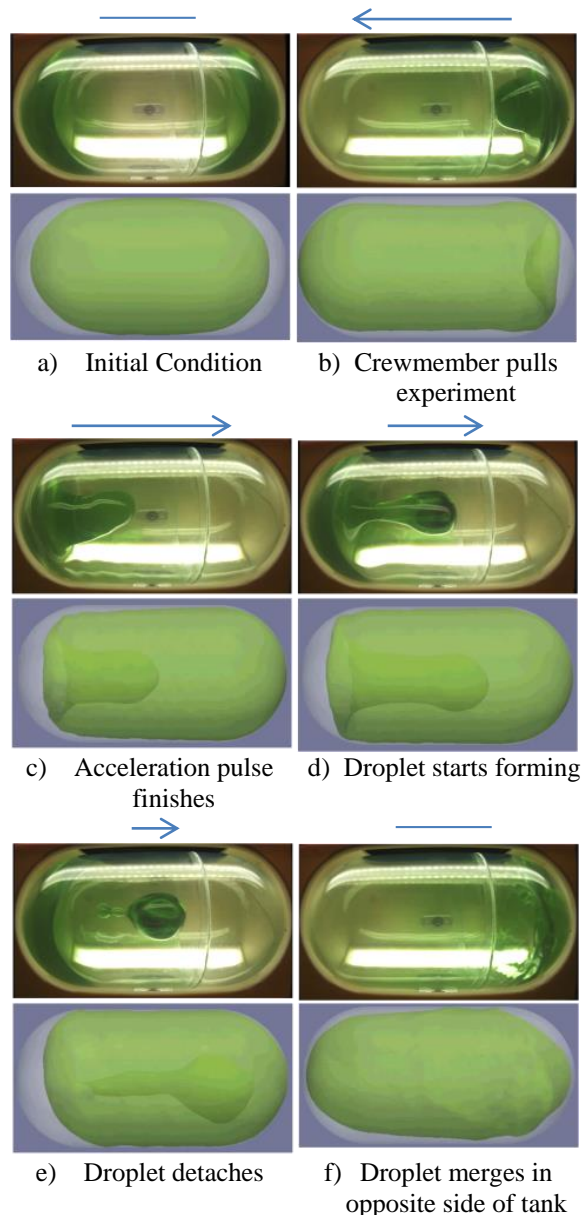


Fig. 4: Simulated satellite deployment

### Tank Spin

Science 3 also included a visual demonstration of surface tension versus inertia dominated regime, as well as rotation about non principal axes and stability. In this demonstration, depicted in Fig. 5a, the crewmember Reid Wiseman provides a spin about the major axis of the tank (minor inertia). The fluid coats the entire inner surface (Fig. 5b), until the rotation starts changing stable axes (Fig. 5c). As the axis changes, the centrifugal force experienced by the fluid increases due to the radius increase, thinning the liquid film (Fig. 5d) and eventually breaking the surface tension (Fig. 5e). A new stable rotation about the minor axis (major moment of inertia)

continues to take place, until the crewmember retrieves the spinning tank (Fig. 5f).

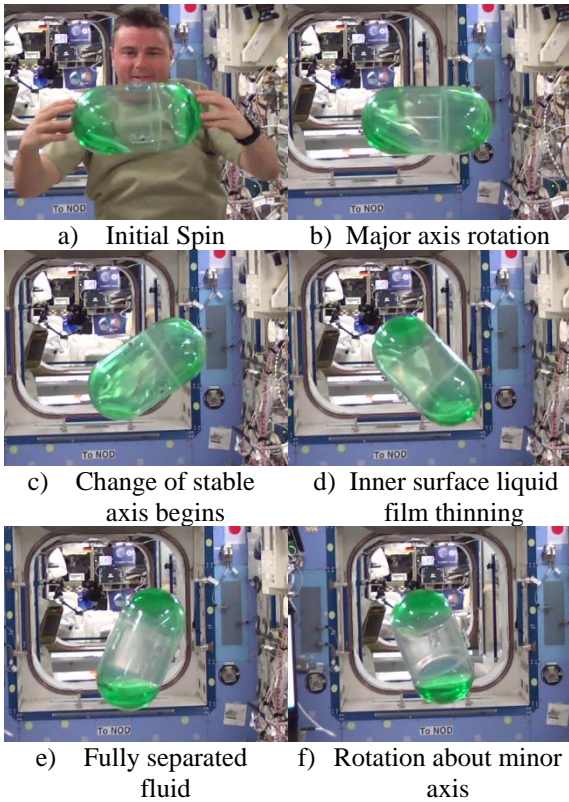


Fig. 5: Surface tension vs inertial dominated regime

Such phenomenon is observed in all space vehicles, requiring spin stabilization in order to rotate about the longitudinal axis. Any energy dissipation, such as viscous forces during fluid motion, and/or unsteady behaviour such as sloshing liquid, will create the conditions necessary to end up in a spin state that minimizes the kinetic rotational energy for a fixed angular momentum (Fig. 6). A clear example of this behaviour was learned from Explorer 1, the first successfully launched U.S. spacecraft. The satellite's spin-stabilized attitude transitioned into a minimum kinetic energy state, a flat spin about its transverse axis,

caused by a vibrating antenna that removed energy from the system. This was deduced from the modulation of the received signal, which produced periodic fade-outs of the signal as the spacecraft tumbled<sup>10</sup>.

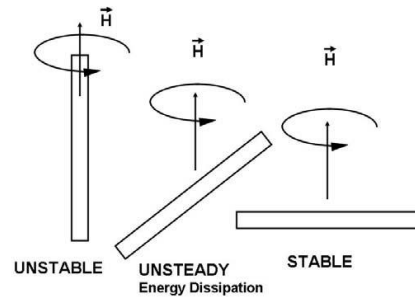


Fig. 6: Unstable and stable axes of rotation<sup>11</sup>

## V. CONCLUSION

This paper provided a snapshot of the current science status and results extracted from the operation of the SPHERES-Slosh Experiment on board the ISS. Chapter III provides a summary of all science sessions performed to date, starting with Checkout and the evolution of initial conditions through Science sessions 1, 2 and 3.

Determination of inertia parameters from actual flight data is presented, matching to CAD parameters with a high uncertainty due to data noise and conditions variability.

CFD simulations using inertial data from Science session 3 as input are compared to actual ISS data and its behaviour discussed. The data is found to have a decent agreement overall, replicating a satellite deployment scenario. A manual tank spin maneuver from Science 3 is also presented and discussed.

The SPHERES-Slosh Experiment opened the door to slosh research on microgravity, with an endless list of improvement possibilities, including the study of liquid acquisition devices, propellant transfer and spacecraft refuelling, as well as research using actual propellants instead of surrogate fluids.

## References

- <sup>1</sup> Berglund, M D, et al. The Boeing Delta IV launch vehicle—Pulse-settling approach for second-stage hydrogen propellant management. s.l. : Acta Astronautica. pp. 416-424. 2.
- <sup>2</sup> Strikwerda, T. E., et al., NEAR Shoemaker: Major anomaly survival, delayed rendezvous and mission success. Breckenridge, CO : Guidance and control 2001, 2001. pp. 597-614. 3.
- <sup>3</sup> Space Exploration Technologies Corporation - Update Archive. SpaceX. [Online] March 2007. [http://www.spacex.com/updates\\_archive.php?page=0107-0707](http://www.spacex.com/updates_archive.php?page=0107-0707).
- <sup>4</sup> SPACEX, Demo Flight 2 -Flight Review Update . s.l. : SPACEX, 2007. <http://www.spacex.com/F1-DemoFlight2-Flight-Review.pdf>.

<sup>5</sup> Acquisition of Long-Duration, Low-Gravity Slosh Data Utilizing Existing ISS Equipment (SPHERES) for Calibration of CFD Models of Coupled Fluid-Vehicle Behavior. Schallhorn, Paul, et al. Denver, CO: s.n., 26-28 Jun. 2012. 1st Annual International Space Station (ISS) Research and Development Conference

<sup>6</sup> Chintalapati, S., Holicker, C, Schulman, R., Contreras, E., Gutierrez, H, and Kirk, D., “Design of an Experimental Platform for Acquisition of Liquid Slosh Data aboard the International Space Station”, 48<sup>th</sup> AIAA/ASME/SAE/ASEE Joint Propulsion Conference, AIAA 2012-4297, 30 July - 01 August 2012, Atlanta, GA

<sup>7</sup> Chintalapati, S., Holicker, C, Schulman, Wise, B., Lapilli, G., Gutierrez, H, and Kirk, D. “Update on SPHERES Slosh for Acquisition of Liquid Slosh Data aboard the ISS”, 49<sup>th</sup> AIAA/ASME/SAE/ASEE Joint Propulsion Conference, AIAA 2013-3903, July 14 - 17, 2013, San Jose, CA

<sup>8</sup> Lapilli, G. et. al, “Design of a liquid sloshing experiment to operate in the International Space Station”, 51<sup>st</sup> AIAA/SAE/ASEE Joint Propulsion Conference, AIAA 10.2514/6.2015-4074, July 27-29, Orlando, FL

<sup>9</sup> Tam, W., Jaekle, Don E., “Design and manufacture of an oxidizer tank with a surface tension PMD”, AIAA 2005-3734

<sup>10</sup> Explorer 1, NSSDC/COSPAR ID: 1958-001A, NASA NSSDC Master Catalog. Online, accessed August 2015.

<sup>11</sup> Peraire, J., Widnall, S., “3D Rigid Body Dynamics: Kinetic Energy; Instability; Equations of Motion”, MIT Open CourseWare, 16.07 Dynamics, Version 2.0, 2008, licensed under CC BY 2.0